

High-contrast ZZ interaction using superconducting qubits with opposite-sign anharmonicity

Peng Zhao,^{1,*} Peng Xu,^{1,2,3} Dong Lan,¹ Ji Chu,¹ Xinsheng Tan,^{1,†} Haifeng Yu,¹ and Yang Yu¹

¹National Laboratory of Solid State Microstructures, School of Physics, Nanjing University, Nanjing 230039, China

²Institute of Quantum Information and Technology, Nanjing University of Posts and Telecommunications, Nanjing, 210003, China

³State Key Laboratory of Quantum Optics and Devices, Shanxi University, Taiyuan, 030006, China

(Dated: July 1, 2022)

For building a scalable quantum processor with superconducting qubits, ZZ interaction is of great concern because its residual has a crucial impact to two-qubit gate fidelity. Two-qubit gates with fidelity meeting the criterion of fault-tolerant quantum computation have been demonstrated using ZZ interaction. However, as the performance of quantum processors improves, the residual static-ZZ can become a performance-limiting factor for quantum gate operation and quantum error correction. Here, we introduce a superconducting architecture using qubits with opposite-sign anharmonicity, a transmon qubit and a C-shunt flux qubit, to address this issue. We theoretically demonstrate that by coupling the two types of qubits, the high-contrast ZZ interaction can be realized. Thus, we can control the interaction with a high on/off ratio to implement two-qubit CZ gates, or suppress it during two-qubit gate operation using XY interaction (e.g., an iSWAP gate). The proposed architecture can also be scaled up to multi-qubit cases. In a fixed coupled system, ZZ crosstalk related to neighboring spectator qubits could also be heavily suppressed.

Engineering a physical system for fault-tolerant quantum computing demands quantum gates with error rates below the fault-tolerant threshold, which has been demonstrated in small-sized superconducting quantum processors [1]. At present, high-performance quantum processors with dozens of superconducting qubits have become available [2], but realizing fault-tolerant quantum computing is still out of reach, mainly because of the heavy overhead needed for error-correction with state-of-the-art gate performance. Therefore, further improving gate performance is essential for realizing fault-tolerant quantum computing with superconducting qubits.

With today's superconducting quantum processors, apart from increasing qubit coherence times, speeding up gates can also fundamentally improve gate performance. However, there is a speed-fidelity trade-off imposed by parasitic interactions. Since the current two-qubit gates typically have lower gate speeds and worse fidelity than single-qubit gates [3], this issue is particularly relevant to two-qubit gates. For implementing a fast two-qubit gates with strong two-qubit coupling, one of the major parasitic interactions is ZZ coupling, which is mostly caused by the coupling between higher energy levels of qubits [4, 5]. Thus, for qubits with weak anharmonicity, such as transmon qubits [6] and C-shunt flux qubits (in single well regions) [7–9], the non-zero parasitic ZZ coupling exists inherently due to the intrinsic energy level diagrams of qubits. This ZZ interaction has been shown to act as a double-edged sword for quantum computing: it can be used to implement high-speed and high-fidelity controlled-Z (CZ) gates [1, 10–12], yet it can also degrade performance of two-qubit gates through XY interaction [2, 8, 11–17]. Moreover, in fixed coupled multi-qubit systems, such as the one shown in Fig.1(a), gate operations in the two qubits enclosed by the rectangle involve six neighboring spectator qubits, and the ZZ coupling related to these qubits cannot be fully turned off by tuning qubits out of resonance [1]. The residual is typically manifested as crosstalk, which results in addressing errors

and phase errors during gate operations and error correction [18–24]. Furthermore, these errors are correlated multi-qubit errors, which are particularly harmful for realizing a fault-tolerant scheme [25]. Given the fidelity and performance limitations related to parasitic ZZ interaction, it is highly desirable to achieve high-contrast control over this parasitic coupling.

To address this challenge, in this work, we introduce a superconducting architecture using qubits with opposite-sign anharmonicity. We theoretically demonstrate our protocol with coupled transmon and C-shunt flux qubits, which have negative and positive anharmonicity, respectively. We show that high-contrast ZZ interaction can be achieved by engineering the system parameters. By utilizing ZZ interaction with a high on/off ratio, we can implement the CZ gate with a speed higher than that of the traditional setup using only one type of qubit (e.g., full transmon systems). Parasitic ZZ coupling can also be deliberately suppressed during two-qubit gate operations using XY interaction (e.g., an iSWAP gate), while leaving the XY interaction completely intact. The proposed architecture can be scaled up to multi-qubit cases, and in fixed coupled systems, ZZ crosstalk related to spectator qubits could also be heavily suppressed.

To start, let us consider a superconducting architecture (hereinafter, the AB-type) where two qubits with opposite-sign anharmonicities are coupled together. The architecture can be treated as a module that can be easily scaled up to multi-qubit case. In Fig. 1(a), we show a case of a nearest-neighbor-coupled qubit lattice, where circles with A and B are two-type qubits with opposite-sign anharmonicities arranged in an -A-B-A-B- pattern. As shown in Fig. 1(b), both qubits can be modeled as a three-level (i.e., $|0\rangle$, $|1\rangle$, $|2\rangle$) anharmonic oscillator for which the Hamiltonian is given as ($\hbar = 1$)

$$H_l = \omega_l q_l^\dagger q_l + \frac{\alpha_l}{2} q_l^\dagger q_l (q_l^\dagger q_l - 1), \quad (1)$$

where the subscript $l = a, b$ labels an anharmonic oscillator with anharmonicity α_l and frequency ω_l , and q_l (q_l^\dagger) is the associated annihilation (creation) operator truncated to the low-

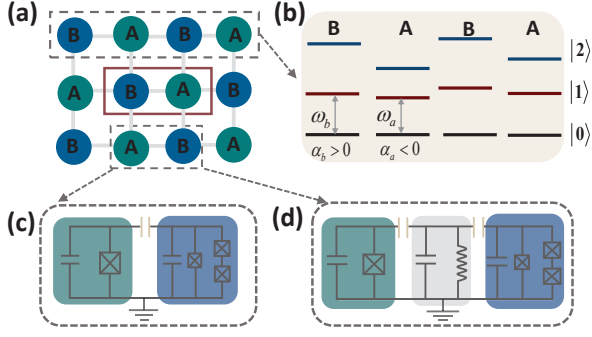


FIG. 1: (a) Layout of a two-dimensional nearest-neighbor lattice, where circles at the vertices denote qubits, and gray lines indicate couplers between adjacent qubits. The lattice consists of two-type qubits arranged in an -A-B-A-B- pattern in each row and column. The circles with A and B are qubits with opposite-sign anharmonicities, and each one can be treated as a three-level anharmonic oscillator (b). Typically, transmon qubits and C-shunt flux qubits can be modeled as anharmonic oscillators with negative and positive anharmonicity, respectively. Qubits can be coupled to each other (c) directly via a capacitor or (d) indirectly using a resonator.

est three-level. Usually, qubits can be coupled directly via a capacitor or indirectly through a bus resonator, as shown in Fig. 1(c) and 1(d). For clarity and without loss of generality, unless explicitly mentioned, we focus on the direct-coupled case in the following discussion, and the dynamics of two-coupled qubits can be described by the Hamiltonian $H = H_a + H_b + H_I$, where $H_I = g(q_a^\dagger q_b + H.c.)$ describes the inter-qubit coupling with strength g .

Before describing our main idea of engineering high-contrast ZZ interaction in our architecture, we need to first examine the origin of parasitic ZZ interaction in the traditional setup (hereinafter, the AA-type), where two transmon qubits are coupled directly. By ignoring higher energy levels, we can model the transmon qubit as an anharmonic oscillator with negative anharmonicity [6], thus the system Hamiltonian can be expressed as H with $\alpha_{a,b} < 0$. Fig. 2(a) shows numerically calculated energy levels of the system for anharmonicities $\alpha_{a,b} = -\alpha$ ($\alpha/2\pi = 250$ MHz, which is a positive number throughout this work) [26]. One can find that there are four avoided crossings, one corresponds to the XY interaction in the one-excitation manifold (i.e., interaction $|01\rangle \leftrightarrow |10\rangle$), and the other three (from left to right) associate with interactions among the two-excitation manifold $\{|11\rangle, |02\rangle, |20\rangle\}$ (i.e., interactions $|11\rangle \leftrightarrow |02\rangle$, $|20\rangle \leftrightarrow |02\rangle$, and $|11\rangle \leftrightarrow |20\rangle$). The interactions between qubit states $|11\rangle$ and non-qubit states ($|02\rangle, |20\rangle$) change the energy of state $|\tilde{11}\rangle$, where $|\tilde{ij}\rangle$ denotes the eigenstate of the Hamiltonian H that has the maximum overlap with the bare state $|ij\rangle$, and the corresponding eigenenergy is $E_{\tilde{ij}}$, thus leading to ZZ coupling with strength

$$\zeta = (E_{\tilde{11}} - E_{\tilde{01}}) - (E_{\tilde{10}} - E_{\tilde{00}}) = J(\tan \frac{\theta_b}{2} - \tan \frac{\theta_a}{2}), (2)$$

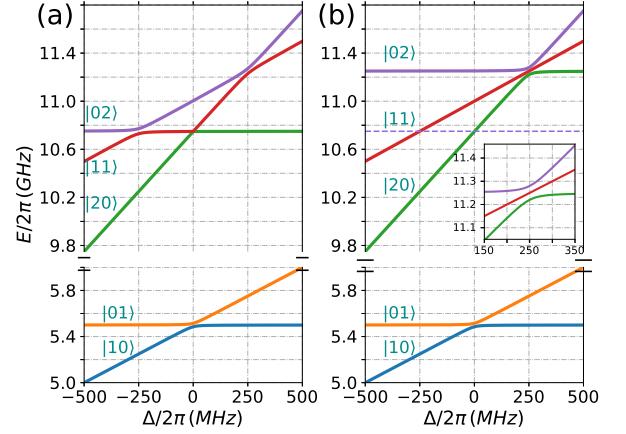


FIG. 2: Numerical calculation of the energy levels of the coupled qubit system as a function of the qubit detuning $\Delta = \omega_a - \omega_b$ for qubit frequency $\omega_b/(2\pi) = 5.5$ GHz, anharmonicity $\alpha/2\pi = 250$ MHz [8, 26], and coupling strength $g/2\pi = 15$ MHz. (a) Qubits with same-sign anharmonicity $\alpha_{a(b)} = -\alpha$; (b) Qubits with opposite-sign anharmonicity $\alpha_{a(b)} = \mp\alpha$. The inset highlights the triple degeneracy point in the two-excitation manifold $\{|02\rangle, |20\rangle, |11\rangle\}$.

where $\tan \theta_{a,b} = 2J/(\Delta \pm \alpha_{a,b})$, $\Delta = \omega_a - \omega_b$ denotes qubit detuning, and $J = \sqrt{2}g$ is the coupling strength of $|11\rangle \leftrightarrow |02\rangle$ ($|20\rangle$). When $J \ll |\Delta \pm \alpha_{a,b}|$, Eq. (2) can be approximated by $\zeta = J^2/(\Delta + \alpha_b) - J^2/(\Delta - \alpha_a)$ [1].

With the expression in Eq. (2), there are two terms contributing to ZZ interaction, and each is independently associated with the interaction $|11\rangle \leftrightarrow |02\rangle$ ($|20\rangle$). Replacing one of the two transmon qubits with a qubit for which the value of anharmonicity is comparable but the sign is positive can destructively interfere the two terms in Eq. (2), thus heavily suppressing ZZ coupling. A promising qubit to implementing such a AB-type setup is the C-shunt flux qubit in single well regime [7–9], where the qubit can be modeled as an anharmonic oscillator that has positive anharmonicity with magnitude comparable to that of the transmon qubit [8, 26]. In Fig. 2(b), we show numerically calculated energy levels for this AB-type setup with $\alpha_b/2\pi = 250$ MHz [8] and keep all other parameters the same as in Fig. 2(a). Compared with the AA-type setup, the avoided crossing associated with interaction $|01\rangle \leftrightarrow |10\rangle$ is completely intact, but the interaction among two-excitation manifold forms an avoided crossing with triplets, as shown in the inset of Fig. 2(b). At the triple degeneracy point, the eigenstates are $(|02\rangle + |20\rangle - \sqrt{2}|11\rangle)/2$, $(|02\rangle - |20\rangle)/\sqrt{2}$, $(|02\rangle + |20\rangle + \sqrt{2}|11\rangle)/2$, with the corresponding energies of $E_{11} - \sqrt{2}J$, E_{11} , and $E_{11} + \sqrt{2}J$ [31].

Fig. 3(a) shows the numerical result of ZZ coupling strength as a function of qubit detuning Δ in the AB-type setup. The result for the AA-type setup is also shown for comparison. In the AB-type setup, ZZ coupling is completely removed away from the triple degeneracy point at $\Delta = \alpha_b$, while for regions close to the degeneracy point, coupling is pre-

served, and the strength at the degeneracy point is larger than that of the AA-type setup ($2g$ vs $\sqrt{2}g$) [31]. In Fig. 3(b), we have also shown ZZ coupling strength as a function of the anharmonicity asymmetry $\delta_\alpha = |\alpha_b| - |\alpha_a|$ for typical coupling strength $g/2\pi = 15$ MHz and qubit detuning $\Delta/2\pi = -150$ MHz. One can find that the ZZ coupling strength is suppressed below 0.7 MHz for the anharmonicity asymmetry around $-100 \sim 600$ MHz. In addition, since the anharmonicities of both types of qubits (the transmon qubit and the C-shunt flux qubit) depend primarily on geometric circuit parameters, the typical anharmonicity asymmetry δ_α around $-20 \sim 20$ MHz could be achieved with current qubit fabrication techniques [26]. In this case, ZZ coupling strength could be further suppressed below 60 KHz, as shown in the inset of Fig. 3(b), whereas for the traditional setup, the typical strength of the residual ZZ coupling is about 5 MHz, as shown in Fig. 3(a).

For a more comprehensive analysis of ZZ coupling in the AB-type setup, we explore the full parameter range in Fig. 3(c) with varying qubit detuning Δ and anharmonicity asymmetry δ_α . We identify three regions in parameter space with prominent characteristic. The two lighter regions indicate that ZZ coupling becomes strong when qubit detuning approaches qubit anharmonicity, i.e., $\Delta = \mp\alpha_{a,b}$, and the intersection region corresponds to the triple degeneracy point. The darker region shows where ZZ coupling is heavily suppressed and is zero for $\delta_\alpha = 0$. In Fig. 3(d), we show the result for an indirect-coupled case, where qubits are coupled via a resonator [32]. In this case, the strength of the effective inter-qubit coupling depends on qubit detuning, thus the zero ZZ coupling point depends not only on the anharmonicity asymmetry, but also on the qubit detuning.

Having shown high contrast ZZ interaction in the AB-type setup, we now turn to study the implementation of two-qubit gates with a diabatic scheme in this setup [4, 11]. Here, we focus on the direct-coupled system with always-on interactions described by the Hamiltonian H with $\alpha_a < 0$ and $\alpha_b > 0$, but the method is generalizable to other coupled systems [32]. For illustration purposes and easy reference, we use the same parameters as those in Fig. 2(b). In this case, during the gate operations, the frequency of qubit b remains at its parking point, while the frequency of qubit a changes from its parking point to the interaction point and then back, according to a time-dependent function [35, 38], as shown in Fig. 4(a) or 4(d) where the full width at half maximum is defined as hold time. We note that at the parking (idling) point where the inter-qubit coupling is effectively turned off, the logical basis state $|\bar{i}\bar{j}\rangle$ is defined as the eigenstates of the system biased at this point [31, 38], which is adiabatically connected to the bare state $|ij\rangle$. Expressed in the logical basis, the target gate operations can be expressed as

$$U(\theta, \phi) = e^{-i(|\bar{0}\bar{1}\rangle\langle\bar{1}\bar{0}| + |\bar{1}\bar{0}\rangle\langle\bar{0}\bar{1}|)\theta} e^{-i|\bar{1}\bar{1}\rangle\langle\bar{1}\bar{1}|\phi}, \quad (3)$$

where θ denotes the swap angle associated with the bare exchange interaction $|01\rangle \leftrightarrow |10\rangle$, and ϕ represents the conditional phase resulting from ZZ coupling. To quantify

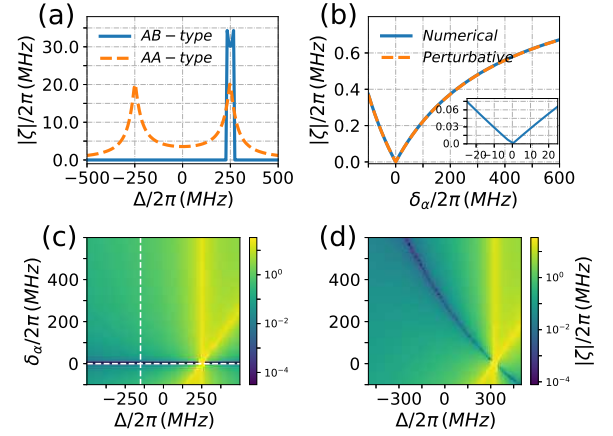


FIG. 3: Numerical results for ZZ coupling strength $|\zeta|$. (a) $|\zeta|$ versus qubit detuning Δ for anharmonicity asymmetry $\delta_\alpha = |\alpha_b| - |\alpha_a| = 0$, where the dashed line shows result for the AA-type. (b) $|\zeta|$ versus δ_α for $\Delta/2\pi = -150$ MHz, where the dashed line shows perturbational result. The inset shows that $|\zeta|$ could be suppressed below 60 KHz with the typical anharmonicity asymmetry ($-20 \sim 20$ MHz). (c) $|\zeta|$ versus Δ and δ_α . Horizontal (vertical) cut through (c) denotes the result plotted in (b). (d) ZZ coupling in a system comprising two qubits that are coupled via a resonator [32].

the intrinsic performance of the implemented gate operation, we use the metric of state-average gate fidelity $F(\theta, \phi) = [\text{Tr}(U^\dagger U) + |\text{Tr}(U(\theta, \phi)^\dagger U)|^2]/20$ [39], where U is the actual evolution operator (ignoring the decoherence process) up to single qubit phase gates.

We first consider the implementation of the CZ gate $U(0, \pi)$, and the main idea is as follows. By tuning the frequency of qubit a from its parking point $\omega_P = 6.1$ GHz to the interaction point $\omega_I = \omega_b + \alpha$ according to the time-dependent function shown in Fig. 4(a), the CZ gate can be realized after a full Rabi oscillation between $|11\rangle$ and $[|02\rangle + |20\rangle]/\sqrt{2}$. As mentioned before, the Rabi rate is larger than in the AA-type setup ($2g$ vs $\sqrt{2}g$), thus allowing a higher gate speed. We note that an additional small overshoot to the interaction frequency ω_I is critical to optimize the leakage to non-qubit states [11, 35]. By taking the optimal overshoot and initializing the system in states $|\bar{1}\bar{1}\rangle$ and $|\bar{0}\bar{1}\rangle$, Fig. 4(b) shows the leakage $\epsilon_{\text{leak}} = 1 - P_{\bar{1}\bar{1}}$ ($P_{\bar{i}\bar{j}}$ denotes the population in the logical state $|\bar{i}\bar{j}\rangle$ at the end of the gate operations) and swap error $\epsilon_{\text{swap}} = 1 - P_{\bar{0}\bar{1}}$ as a function of the hold time. In present system with fixed inter-qubit coupling, it is nearly impossible to have an optimal hold time to simultaneously minimize the swap error and leakage, as shown in Fig. 4(b). Thus, here, we choose to minimize the leakage, and find that with a hold time of 17.3 ns, a CZ gate with fidelity above 99.999% can be achieved, and both the leakage and swap error can be suppressed to below 10^{-4} . However, as shown in Fig. 4(c), when the system is considered with typical anharmonicity asymmetry δ_α , gate fidelity worsens. In order to identify the performance limiting factors, we extract phase error δ_θ , δ_ϕ with re-

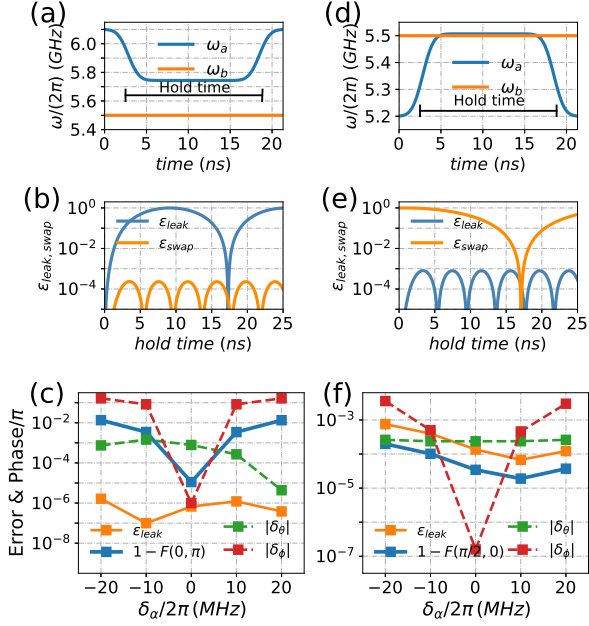


FIG. 4: Numerical results for CZ gate and iSWAP gate implementation in our architecture. The system parameters used are same as in Fig. 2(b). (a),(d) Typical pulses with small overshoots for realizing CZ gates and iSWAP gates, where the full width at half maximum is defined as hold time. (b),(e) Leakage ϵ_{leak} and swap error ϵ_{swap} versus hold time for system with anharmonicity asymmetry $\delta_\alpha = 0$ and optimal overshoots [35]. (c),(f) Gate error $1 - F$ versus typical anharmonicity asymmetry. The phase error $\delta_\theta, \delta_\phi$ with respect to the ideal phase parameters $(0, \pi)$ for CZ gate, and $(\pi/2, 0)$ for iSWAP gate) and leakage error ϵ_{leak} are also presented for identifying the major source of error.

spect to the ideal phase parameters $\theta = 0, \phi = \pi$ for CZ gate and the leakage, and find that in the current case, gate error primarily result from conditional phase error δ_ϕ . This can be explained by the fact that in systems with typical anharmonicity asymmetry, the resonance condition for having a full Rabi oscillation between $|11\rangle$ and non-qubit state breaks down. Off-resonance Rabi oscillation is thus presented, causing conditional phase error [35].

An iSWAP gate $U(\pi/2, 0)$ can be realized by tuning the two qubits into resonance according to the control pulse shown in Fig. 4(d). Given an optimal overshoot with respect to the interaction point $\omega_a = \omega_b$, an iSWAP gate with fidelity exceeding 99.99% can be realized with a hold time of 17.1 ns [40], and leakage ϵ_{leak} and swap error $\epsilon_{\text{swap}} = P_{01}$ can be suppressed to below 10^{-4} , as shown in Fig. 4(e). As shown in Fig. 4(f), we also study the effect of anharmonicity asymmetry on gate fidelity, and find that gate fidelity in excess of 99.98% can be achieved for system with typical anharmonicity asymmetry. By extracting phase error $\delta_\theta, \delta_\phi$ and leakage for the iSWAP gate, we find that leakage error becomes the major source of error. Finally, we note that apart from leakage and swap error, phase error δ_ϕ resulted from parasitic ZZ coupling

limits the performance of iSWAP gates in the traditional AA-type setup [2, 11, 12]. The high-fidelity iSWAP gate and the low conditional phase error δ_ϕ demonstrated above indicate that parasitic ZZ coupling is indeed heavily suppressed in the AB-type setup.

In summary, we have studied parasitic ZZ coupling in a superconducting architecture [41–43] where two qubits with opposite-sign anharmonicities are coupled together and found that high-contrast control over parasitic ZZ coupling can be realized. We further show that CZ gates with higher gate speed and iSWAP gates with dramatically lower conditional phase error can be realized with diabatic schemes in the proposed architecture. Moreover, as shown in Fig. 4(b) and 4(c), XY gates with arbitrary swap angles [44], leakage error below 10^{-3} , and negligible phase error is achievable, as is arbitrary control phase gate with swap error below 10^{-3} . Since these errors are caused by off-resonant Rabi oscillation related to the associated parasitic interaction (i.e., $|01\rangle \leftrightarrow |10\rangle$ for CZ gates, and $|11\rangle \leftrightarrow |20\rangle$ ($|02\rangle$) for iSWAP gates), even lower error rates should be possible by increasing the value of anharmonicity [43] or using the synchronization procedure [11]. Implementing these continuous set of gates natively could be useful for near-term applications of quantum processors [12, 44]. As one may expect, the high-contrast control over ZZ coupling could also improve the performance of parametric activated gates [15–17] and cross-resonance gates [8, 14]. In multi-qubit systems and with fixed coupled cases, the crosstalk resulted from ZZ coupling could be heavily suppressed, thus, gate operations can be implemented simultaneously with low crosstalk. For tunable coupled cases [45–48], XY gates with arbitrary swap angles can be implemented natively with negligible conditional phase error [2, 11, 12].

We would like to thank Songy for helpful suggestion on the manuscript. This work was partly supported by the NKRD of China (Grant No. 2016YFA0301802), NSFC (Grant No. 61521001, and No. 11890704), and the Key R&D Program of Guangdong Province (Grant No.2018B030326001). P. X acknowledges the supported by Scientific Research Foundation of Nanjing University of Posts and Telecommunications (NY218097), NSFC (Grant No. 11847050), and the Young fund of Jiangsu Natural Science Foundation of China (Grant No. BK20180750). Haifeng Yu acknowledges support from the BJNSF (Grant No.Z190012).

* Electronic address: shangniguo@sina.com

† Electronic address: meisen0103@163.com

- [1] R. Barends, J. Kelly, A. Megrant, A. Veitia, D. Sank, E. Jeffrey, T. C. White, J. Mutus, A. G. Fowler, B. Campbell, Y. Chen, Z. Chen, B. Chiaro, A. Dunsworth, C. Neill, P. O’Malley, P. Roushan, A. Vainsencher, J. Wenner, A. N. Korotkov, A. N. Cleland, and J. M. Martinis, Superconducting quantum circuits at the surface code threshold for fault tolerance, *Nature* **508**, 500 (2014).
- [2] F. Arute, K. Arya, R. Babbush, D. Bacon, J. C. Bardin, R.

- Barends, R. Biswas, S. Boixo, F. G. Brandao, D. A. Buell, et al., Quantum supremacy using a programmable superconducting processor, *Nature* **574**, 505 (2019).
- [3] M. Kjaergaard, M. E. Schwartz, J. Braumüller, P. Krantz, J. I.-J. Wang, S. Gustavsson, and W. D. Oliver, Superconducting qubits: Current state of play, [arXiv:1905.13641](https://arxiv.org/abs/1905.13641) (2019).
- [4] F. W. Strauch, P. R. Johnson, A. J. Dragt, C. J. Lobb, J. R. Anderson, and F. C. Wellstood, Quantum Logic Gates for Coupled Superconducting Phase Qubits, *Phys. Rev. Lett.* **91**, 167005 (2003).
- [5] L. DiCarlo, J. M. Chow, J. M. Gambetta, L. S. Bishop, B. R. Johnson, D. I. Schuster, J. Majer, A. Blais, L. Frunzio, S. M. Girvin, and R. J. Schoelkopf, Demonstration of two-qubit algorithms with a superconducting quantum processor, *Nature (London)* **460**, 240 (2009).
- [6] J. Koch, T. M. Yu, J. Gambetta, A. A. Houck, D. I. Schuster, J. Majer, A. Blais, M. H. Devoret, S. M. Girvin, and R. J. Schoelkopf, Charge-insensitive qubit design derived from the cooper pair box, *Phys. Rev. A* **76**, 042319 (2007).
- [7] M. Steffen, S. Kumar, D. P. DiVincenzo, J. R. Rozen, G. A. Keefe, M. B. Rothwell, and M. B. Ketchen, High-Coherence Hybrid Superconducting Qubit, *Phys. Rev. Lett.* **105**, 100502 (2010).
- [8] J. M. Chow, A. D. Córcoles, J. M. Gambetta, C. Rigetti, B. R. Johnson, J. A. Smolin, J. R. Rozen, G. A. Keefe, M. B. Rothwell, M. B. Ketchen, and M. Steffen, Simple All-Microwave Entangling Gate for Fixed-Frequency Superconducting Qubits, *Phys. Rev. Lett.* **107**, 080502 (2011).
- [9] F. Yan, S. Gustavsson, A. Kamal, J. Birenbaum, A. P. Sears, D. Hover, T. J. Gudmundsen, D. Rosenberg, G. Samach, S. Weber, J. L. Yoder, T. P. Orlando, J. Clarke, A. J. Kerman, and W. D. Oliver, The flux qubit revisited to enhance coherence and reproducibility, *Nat. Commun.* **7**, 12964 (2016).
- [10] M. A. Rol, F. Battistel, F. K. Malinowski, C. C. Bultink, B. M. Tarasinski, R. Vollmer, N. Haider, N. Muthusubramanian, A. Bruno, B. M. Terhal et al., A Fast, Low-Leakage, High-Fidelity Two-Qubit Gate for a Programmable Superconducting Quantum Computer, *Phys. Rev. Lett.* **123**, 120502 (2019)
- [11] R. Barends, C. M. Quintana, A. G. Petukhov, Y. Chen, D. Kafri, et al., Diabatic Gates for Frequency-Tunable Superconducting Qubits, *Phys. Rev. Lett.* **123**, 210501 (2019).
- [12] B. Foxen, C. Neill, A. Dunsworth, P. Roushan, B. Chiaro, et al., Demonstrating a Continuous Set of Two-qubit Gates for Near-term Quantum Algorithms, [arXiv:2001.08343](https://arxiv.org/abs/2001.08343) (2020).
- [13] S. Sheldon, E. Magesan, J. M. Chow, and J. M. Gambetta, Procedure for systematically tuning up cross-talk in the cross-resonance gate, *Phys. Rev. A* **93**, 060302(R) (2016).
- [14] A.D. Patterson, J. Rahamim, T. Tsunoda, P.A. Spring, S. Jebari, K. Ratter, M. Mergenthaler, G. Tancredi, B. Vlastakis, M. Esposito, and P.J. Leek, Calibration of a Cross-Resonance Two-Qubit Gate Between Directly Coupled Transmons, *Phys. Rev. Applied* **12**, 064013 (2019)
- [15] D. C. McKay, S. Filipp, A. Mezzacapo, E. Magesan, J. M. Chow, and J. M. Gambetta, Universal gate for fixed-frequency qubits via a tunable bus, *Phys. Rev. Applied* **6**, 064007 (2016).
- [16] M. Reagor, C. B. Osborn, N. Tezak, A. Staley, et al., Demonstration of universal parametric entangling gates on a multi-qubit lattice, *lattice. Sci. Adv.* **4**, eaao3603 (2018).
- [17] S. A. Caldwell, N. Didier, C. A. Ryan, E. A. Sete, A. Hudson, et al., Parametrically Activated Entangling Gates Using Transmon Qubits, *Phys. Rev. Applied* **10**, 034050 (2018).
- [18] J. M. Gambetta, A. D. Córcoles, S. T. Merkel, B. R. Johnson, J. A. Smolin, J. M. Chow, C. A. Ryan, C. Rigetti, S. Poletto, T. A. Ohki, M. B. Ketchen, and M. Steffen, Characterization of Addressability by Simultaneous Randomized Benchmarking, *Phys. Rev. Lett.* **109**, 240504 (2012).
- [19] D. C. McKay, S. Sheldon, J. A. Smolin, J. M. Chow, and J. M. Gambetta, Three Qubit Randomized Benchmarking, *Phys. Rev. Lett.* **122**, 200502 (2019).
- [20] M. Takita, A. W. Cross, A. D. Córcoles, J. M. Chow, and J. M. Gambetta, Experimental Demonstration of Fault-tolerant State Preparation with Superconducting Qubits, *Phys. Rev. Lett.* **119**, 180501 (2017).
- [21] M. Takita, A. D. Córcoles, E. Magesan, B. Abdo, M. Brink, A. Cross, J. M. Chow, and J. M. Gambetta, Demonstration of Weight-Four Parity Measurements in the Surface Code Architecture, *Phys. Rev. Lett.* **117**, 210505 (2016).
- [22] C. K. Andersen, A. Remm, S. Balasiu, S. Krinner, J. Heinsoo, J. Besse, M. Gabureac, A. Wallraff, and C. Eichler, Entanglement Stabilization using Parity Detection and Real-Time Feedback in Superconducting Circuits, [arXiv:1902.06946](https://arxiv.org/abs/1902.06946) (2019).
- [23] C. C. Bultink, T. E. O'Brien, R. Vollmer, N. Muthusubramanian, M. W. Beekman, M. A. Rol, X. Fu, B. Tarasinski, V. Ostroukh, B. Varbanov, A. Bruno, L. DiCarlo, Protecting quantum entanglement from qubit errors and leakage via repetitive parity measurements, [arXiv:1905.12731](https://arxiv.org/abs/1905.12731) (2020).
- [24] C. K. Andersen, A. Remm, S. Lazar, S. Krinner, N. Lacroix, G. J. Norris, M. Gabureac, C. Eichler, and A. Wallraff, Repeated Quantum Error Detection in a Surface Code, [arXiv:1912.09410](https://arxiv.org/abs/1912.09410) (2020).
- [25] A. G. Fowler, M. Mariantoni, J. M. Martinis, and A. N. Cleland, Surface codes: Towards practical large-scale quantum computation, *Phys. Rev. A* **86**, 032324 (2012).
- [26] See Supplemental Material: Circuit Hamiltonian, which includes Refs.[27–30].
- [27] J. Q. You, X. Hu, S. Ashhab, and F. Nori, Low-decoherence flux qubit, *Phys. Rev. B* **75**, 140515(R) (2007).
- [28] U. Vool and M. Devoret, Introduction to quantum electromagnetic circuits, *Int. J. Circuit Theory Appl.* **45**, 897 (2017).
- [29] J. Kelly, R. Barends, A. G. Fowler, A. Megrant, E. Jeffrey, T. C. White, D. Sank, J. Y. Mutus, B. Campbell, Yu Chen, Z. Chen, B. Chiaro, A. Dunsworth, I.-C. Hoi, C. Neill, P. O'Malley, C. Quintana, P. Roushan, A. Vainsencher, J. Wenner, A. N. Cleland, and John M. Martinis, State preservation by repetitive error detection in a superconducting quantum circuit, *Nature* **519**, 66 (2015).
- [30] O. Heinsoo, C. K. Andersen, A. Remm, S. Krinner, T. Walter, Y. Salathé, S. Gasparinetti, J.-C. Besse, A. Potočník, A. Wallraff, and C. Eichler, Rapid high-fidelity multiplexed readout of superconducting qubits, *Phys. Rev. Applied* **10**, 034040 (2018).
- [31] See Supplemental Material: Triple degeneracy point.
- [32] See Supplemental Material: Qubit coupled via a coupler, which includes Refs.[33, 34].
- [33] R. Krishnan and J. A. Pople, Approximate fourth-order perturbation theory of the electron correlation energy, *Int. J. Quantum Chem.* **14**, 91 (1978).
- [34] R. Winkler, Spin-Orbit Coupling Effects in Two-Dimensional Electron and Hole System (Springer, 2003).
- [35] See Supplemental Material: Gate operation with diabatic scheme, which includes Refs.[36, 37].
- [36] E. Zahedinejad, J. Ghosh, and B. C. Sanders, Designing High-Fidelity Single-Shot Three-Qubit Gates: A Machine-Learning Approach, *Phys. Rev. Applied* **6**, 054005 (2016).
- [37] E. Barnes, C. Arenz, A. Pitchford, and S. E. Economou, Fast microwave-driven three-qubit gates for cavity-coupled superconducting qubits, *Phys. Rev. B* **96**, 024504 (2017).
- [38] J. Ghosh, A. Galiatdinov, Z. Zhou, A. N. Korotkov, J. M. Martinis, and M. R. Geller, High-fidelity controlled- σ^Z

- gate for resonator-based superconducting quantum computers, *Phys. Rev. A* **87**, 022309 (2013).
- [39] L. H. Pedersen, N. M. Møller, and K. Mølmer, Fidelity of quantum operations, *Phys. Lett. A* **367**, 47 (2007).
- [40] We note that similar to the CZ gate case, it is nearly impossible to simultaneously minimize the swap error and leakage for iSWAP gates in present system with fixed coupling strength, as shown in Fig. 4(e). In present work, hold time is chosen to minimize the swap error for the implementation of the iSWAP gate.
- [41] Two theoretical superconducting architectures with multi-type qubits were previously proposed, but they address different challenges [42, 43]. In the work of M. Elliott *et al.* [42], two qubits with opposite anharmonicities are coupled to a cavity to achieve cancelation of the cavity self-Kerr effect. In the work of E. A. Sete *et al.* [43], transmon qubits are coupled to fluxonium in a lattice with an -A-B-A-B- pattern, where ZZ coupling resulted from the interaction between $|11\rangle$ and $|02\rangle$ (Here the first digit denotes the transmon states and the second one denotes the fluxonium states) is suppressed by the strong fluxonium anharmonicity, while the contribution of the interaction between $|11\rangle$ and $|20\rangle$ is preserved.
- [42] M. Elliott, J. Joo, and E. Ginossar, Designing Kerr interactions using multiple superconducting qubit types in a single circuit, *New. J. Phys.* **20**, 023037 (2018).
- [43] E. A. Sete, W. J. Zeng, and C. T. Rigetti, A functional architecture for scalable quantum computing, 2016 IEEE International Conference on Rebooting Computing (ICRC). *IEEE*, 2016: 1-6.
- [44] D. M. Abrams, N. Didier, B. R. Johnson, M. P. da Silva, C. A. Ryan, Implementation of the XY interaction family with calibration of a single pulse, [arXiv:1912.04424](https://arxiv.org/abs/1912.04424) (2019).
- [45] Y. Chen, C. Neill, P. Roushan, N. Leung, M. Fang, R. Barends, J. Kelly, B. Campbell, Z. Chen, B. Chiaro, A. Dunsworth, E. Jeffrey, A. Megrant, J. Y. Mutus, P. J. J. O'Malley, C. M. Quintana, D. Sank, A. Vainsencher, J. Wenner, T. C. White, M. R. Geller, A. N. Cleland, and J. M. Martinis, Qubit architecture with high coherence and fast tunable coupling, *Phys. Rev. Lett.* **113**, 220502 (2014).
- [46] C. Neill. A path towards quantum supremacy with superconducting qubits. PhD thesis, University of California Santa Barbara, Dec 2017.
- [47] F. Yan, P. Krantz, Y. Sung, M. Kjaergaard, D. L. Campbell, T. P. Orlando, S. Gustavsson, and W. D. Oliver, Tunable Coupling Scheme for Implementing High-Fidelity Two-Qubit Gates, *Phys. Rev. Applied* **10**, 054062 (2018).
- [48] P. S. Mundada, G. Zhang, T. Hazard, and A. A. Houck, Suppression of Qubit Crosstalk in a Tunable Coupling Superconducting Circuit, *Phys. Rev. Applied* **12**, 054023 (2019).